Mean Lifetime of the π^0 Meson

D. A. EVANS
Nuclear Physics Laboratory, University of Oxford, Oxford, England
(Received 15 March 1965)

An experiment is described to measure the mean life of the π^0 meson using nuclear emulsions. The basic method has also been employed by other workers in recent years, viz., the determination of the flight distances of π^0 mesons produced at a unique velocity in the $K_{\pi 2}$ decay mode of the K^+ meson and decaying through the mode $\pi^0 \rightarrow \gamma e^+ e^-$. The coordinates of the grains composing the tracks in 67 such events were measured and the flight distances of the π^0's determined by geometrical reconstruction of the events. It was considered that an accurate estimation of the various errors involved was essential to the correct computation of the lifetime and such estimations were attempted. The effect of the presence of a certain type of spurious event upon the final results is demonstrated. The value for the mean lifetime obtained is $\tau_{\pi^0} = (1.6_{-0.5}{}^{/+0.6}) \times 10^{-16}$ sec.

INTRODUCTION

In recent years, several determinations—as opposed to a larger number of earlier experiments which set a series of decreasing upper limits—of the mean life of the π^0 meson have been reported, all of which use nuclear emulsions.[1–4] With one exception,[4] the basic method is that due to Harris *et al.*[5] The π^0 is produced at a unique velocity in the $K_{\pi 2}$ decay mode (at rest) of the K^+ meson ($K^+ \rightarrow \pi^+ \pi^0$). The decay of the π^0 is detected by the comparatively infrequent "Dalitz" decay mode (branching ratio $\sim 1.2\%$) involving the "internal conversion" of one of the decay photons to an electron pair, commonly called a "Dalitz pair."[6] An illustration of the appearance of a typical event (hereafter called *KD* event) is given in Fig. 1. The flight distance of the π^0 is inferred either from camera lucida drawings of the events or by some form of grain coordinate measurements with subsequent track fitting.

The results quoted are as follows (in units of 10^{-16} sec): Glasser *et al.*[1] 1.9 ± 0.5; Tietge and Püschel[2] $2.3_{-1.0}{}^{+1.1}$; Koller *et al.*[3] 2.8 ± 0.9. Shwe *et al.*,[4] using high-energy π^0's produced in 3.5-GeV/c π^- interactions with emulsion nuclei, but otherwise employing a technique of grain-coordinate measurement, obtained a value of $(1.7 \pm 0.5) \times 10^{-16}$ sec. These results are to be contrasted with a lifetime of $(1.05 \pm 0.18) \times 10^{-16}$ sec recently obtained by von Dardel *et al.*[7] using counter technique and an entirely new approach to the problem.

In this paper the results are presented of an experiment to measure the lifetime of the π^0; the method used is again basically that of Harris *et al.*[5] The results are intended to replace those of Blackie *et al.*[8] which were obtained using the same emulsion stack. This experiment uses all the events employed by Blackie *et al.* in addition to new ones found by further scanning. However, a refined technique of measurement is used and the method of evaluating the results has been carefully examined together with a close appraisal of the main sources of error. An attempt has been made to estimate the magnitudes of the errors with some precision.

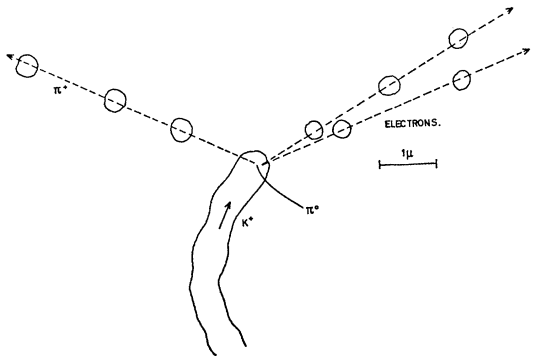

FIG. 1. Appearance of typical *KD* event.

EXPOSURE AND SCANNING

A stack of 200 pellicles of Ilford L4 emulsion was exposed to a 700-MeV/c K^+ beam at the Berkeley Bevatron. The dimensions of each pellicle were 8 in. $\times 6$ in. $\times 400\,\mu$. The momentum of the beam was degraded to 400 MeV/c so that the great majority of K^+'s came to rest in the center of the stack.

After processing, an area scan was carried out in the region of greatest density of stopped K's. A total of 70 000 K^+ decays were examined. This yielded 103 candidates for the desired events of $K_{\pi 2}$ decay with a subsequent decay of the π^0 in the Dalitz mode (*KD* events).

The scanning criteria were such that some contamination is present from the three-body decay modes of the K^+ in which a π^0 is produced and there is only a single charged secondary, viz., $K_{\pi 3}'(\tau') \rightarrow \pi^+ \pi^0 \pi^0$;

[1] R. G. Glasser, N. Seeman, and B. Stiller, Phys. Rev. **123**, 1014 (1961).
[2] J. Tietge and W. Püschel, Phys. Rev. **127**, 1324 (1962).
[3] E. L. Koller, S. Taylor, and T. Huetter, Nuovo Cimento **27**, 1405 (1963).
[4] H. Shwe, F. M. Smith, and W. H. Barkas, Phys. Rev. **136**, B1839 (1964).
[5] G. Harris, J. Orear, and S. Taylor, Phys. Rev. **106**, 327 (1957).
[6] R. H. Dalitz, Proc. Phys. Soc. (London) **A64**, 667 (1951).
[7] G. von Dardel, D. Dekkers, R. Mermod, J. D. van Putten, M. Vivargent, G. Weber, and K. Winter, Phys. Letters **4**, 51 (1963).
[8] R. F. Blackie, A. Engler, and J. H. Mulvey, Phys. Rev. Letters **5**, 384 (1960).

$K_{\mu 3} \rightarrow \mu^+\pi^0\nu_\mu$; $K_{e3} \rightarrow e^+\pi^0\nu_e$. The branching ratios of these modes are, respectively, 2.1%, 4.4%, and 4.5%, while that of the $K_{\pi 2}$ mode is 25.6%.[9] This gives a total expected contamination of about 34%.[10]

The contamination was reduced by measuring the grain density of the charged secondary track. The π^+ emitted in the τ' mode always has $g^* \gtrsim 1.4$ and this mode is easily rejected. The energy spectrum of the μ^+ in the $K_{\mu 3}$ mode extends into the minimum ionizing region but by rejecting tracks with $g^* > 1.4$, about 30% of the $K_{\mu 3}$ decays are expected to be eliminated, which, together with the τ' decays, reduces the total contamination to about 23%. A correction for the remaining $K_{\mu 3}$ and K_{e3} decays was applied later to the final value of lifetime obtained.

Of the original 103 candidates, 19 were rejected on the basis of grain-density measurements.[11] A further selection was made on the basis of the dip angles of the tracks in each event. Those events in which the dip of any track exceeded $50\,\mu/100\,\mu$ (in the processed emulsion) were rejected. This left a final sample of 67 events which were considered suitable for measurement.

METHOD OF MEASUREMENT

The idealized geometry of an event is shown in Fig. 2. For the sake of clarity, only one electron of the Dalitz pair is shown.

The trajectories of the charged particles are determined by measuring the (x,y) coordinates (relative to some arbitrary fixed origin in the emulsion) of the grains composing the tracks and fitting to them the "best" straight lines. The coordinates of the estimated center of the last grain of the K^+ track are also measured. From these data a geometrical reconstruction of the event may be made and the flight distance of the π^0 measured.

The following definitions are made:

(i) The "point of production" of the π^0 (or decay point of the K^+) is the foot of the perpendicular from the measured K^+ ending co-ordinate on to the line of the π^+ track.

(ii) The "point of decay" of the π^0 is at the intersection of the trajectories of the π^+ and one electron.

(iii) The sign of the flight distance is taken to be positive if the decay point as defined in (ii) lies on the opposite side of the production point from the physically existing π^+ track (as distinct from the whole line of the trajectory).

The measurements of the grain coordinates were carried out on a Koristka R4 microscope fitted with a specially constructed bifilar micrometer eyepiece. A full description of the instrument is given elsewhere.[12] It may be noted here, however, that an unusual feature is that the motions of both crosswires are digitized using moire-fringe technique with linear gratings. Each grating and its corresponding crosswire are mounted together on a metal slide so that there is no backlash present in any measurement. The coded coordinates of each grain are automatically punched on to five-hole computer tape and this enables rapid measurement of events. The design of the cross-wires is also unconventional; each consists of two parallel lines with a separation such that the image of a grain of average diameter ($\sim 0.3\,\mu$) just fills the gap between the lines when the normal measuring magnification ($\times 1500$–2000) is used. At the intersection of the crosswires a "box" is formed and the crosswires are adjusted to enclose the grain in the box. As there is no obscuration of the image, even faint grains could be measured. The over-all precision of the equipment was estimated by repeated measurements on the same set of grains. The standard deviation in one coordinate reading (x or y) representing a single measurement on one grain was found to be $\sim 0.05\,\mu$.

The main body of the microscope is encased in an aluminum box lined with expanded polystyrene sheeting

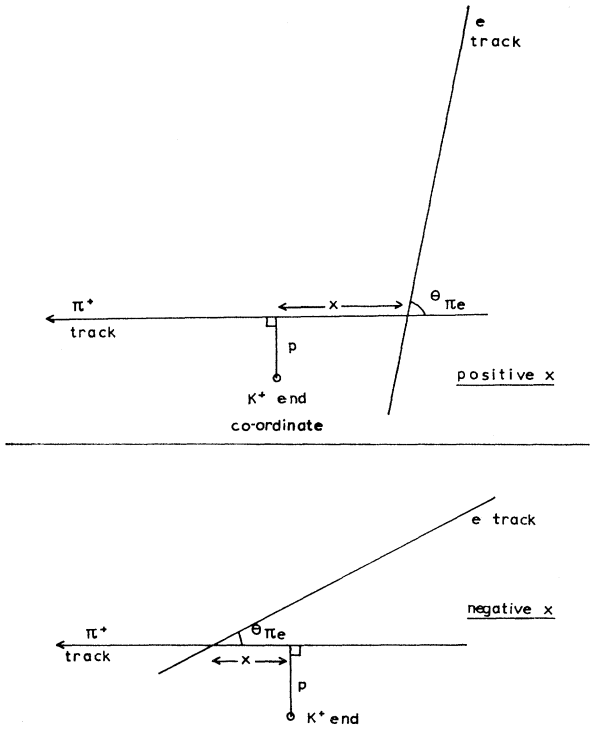

FIG. 2. Reconstructed event showing geometry and quantities calculated.

[9] F. S. Crawford, *Proceedings of the 1962 Annual International Conference on High Energy Physics at Rochester* (Interscience Publishers, Inc., New York, 1962), p. 838.

[10] The τ' mode is doubly weighted as either π^0 may produce a Dalitz pair.

[11] In fair agreement with a figure of 15 predicted from the branching ratios.

[12] D. A. Evans and F. Foster, Nucl. Instr. Methods **30**, 93 (1964).

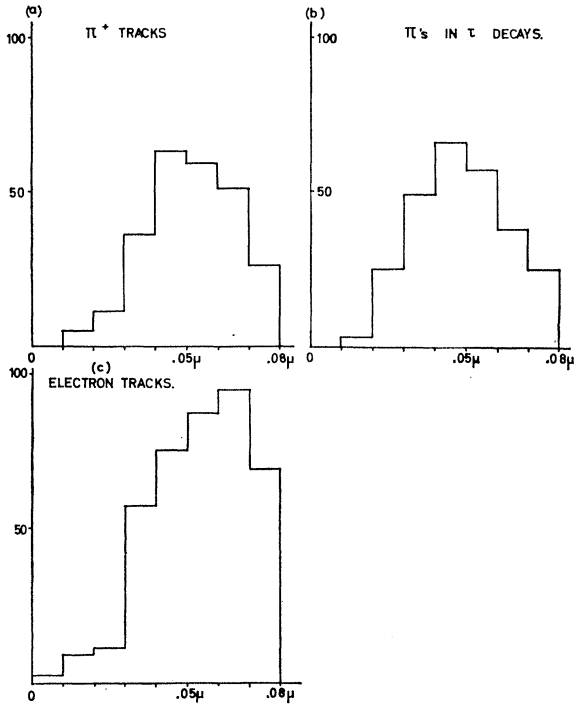

FIG. 3. Distributions of δ_{rms}, the root mean square of the deviations of the measured grain positions from the fitted straight line (a) π^+ tracks in KD events; (b) π tracks in τ events; (c) electrons in KD events.

to provide shielding from external temperature variations. Without the box, it was found that the expansion of the microscope under the diurnal temperature variation caused considerable drifting of the image relative to the field of view. With the thermal shield in place, the drift during a single measurement of an event is found to be negligible. The short time in which a measurement can be completed ($\sim$5 min) due to the digitization of the eyepiece, also assists the reduction of the effect of any residual thermal drift.

The order of measuring the grains of an event was standardized as follows:

(i) π^+ track, proceeding from the edge of the field of view in towards the K^+ ending,

(ii) the K^+ ending,

(iii) one electron track, proceeding outwards from the K^+ ending,

(iv) the other electron track (if measurable[13]), proceeding inwards towards the K^+ ending.

This routine minimized the effect of any remaining drift and also required the least unnecessary movement of the filars. Only the grains within the field of view ($\sim 50\,\mu$ diameter) were measured; this gave from about 6 to about 15 grains in each track (depending upon ionization, dip, and magnification). Each event was measured independently four times, all measurements being performed by the author.

[13] In some cases only one electron track was suitable for measurement as the other had either very few grains or was indistinguishable from the first except at larger distances (more than one field of view).

DATA ANALYSIS

The trajectory of each track is calculated by fitting a straight line to the set of measured grain coordinates such that the quantity

$$P^2=\sum_i^N \frac{(y_i-mx_i-c)^2}{1+m^2}$$

(where N is the number of grains) is a minimum. P^2 is the sum of the squares of the perpendiculars from the points (x_i,y_i) on to the line $y=mx+c$. This method of fitting is logically suited to the present case by considering a simple view of track formation. Furthermore, the x_i's and y_i's are treated symmetrically, unlike the usual form of least-squares fit which merely minimizes

$$P'^2=\sum_{i=1}^N (y_i-mx_i-c)^2.$$

This latter method fails for large values of m.

No explicit account is taken of the different effects causing the measured coordinates to deviate from a true straight line, e.g., measurement error, "grain noise," and multiple scattering. The size of $(P^2)_{\text{min}}$ is a measure of the closeness of fit [$(P^2)_{\text{min}}=0$ for a perfect fit]. A useful related quantity is δ_{rms} defined as $\delta_{\text{rms}}^2=(P^2)_{\text{min}}/N$, where N is the number of grains in the track. δ_{rms} is in fact the root-mean-square deviation of the measured grain positions from the calculated trajectory. Figure 3 shows the distributions obtained for δ_{rms} in various types of track. In all cases it is seen that there is a cutoff above $0.08\,\mu$. This cutoff was imposed in the fitting procedure. If δ_{rms} exceeded $0.08\,\mu$, the "worst"-fitting grain was rejected and the line refitted. This was repeated until δ_{rms} was less than $0.08\,\mu$. This routine was mainly intended to reject spurious grains which had been inadvertently included during measurement.[14] It is seen that the two distributions for π^+ tracks from KD events and τ events (also measured for error calculations) are very similar indicating that the expected extra scattering of the lower energy π's from the τ decays does not affect the distribution of δ_{rms} significantly. It seems likely, therefore, that the distribution of δ_{rms} is due to measurement error and "grain noise" alone for the π tracks. The distribution of δ_{rms} for the electron tracks, however, does indicate the effect of scattering in the greater tendency towards larger values of δ_{rms}.

The following quantities are calculated using the fitted equations of the tracks:

(i) x, the apparent flight distance of the π^0 (in μ);

[14] With a steep track, extrapolation by eye to detect the next grain could include such spurious grains.

(ii) $\csc^2\theta_{\pi e}$ ($\theta_{\pi e}$ is the angle between the π^+ track and the electron track);

(iii) p, the length of the perpendicular from the measured K^+ decay point on to the π^+ track;

(iv) $\sigma_{\pi e}$, the error in x due to the uncertainty in the line fitting (caused by the finite values of δ_{rms} for each track).

In general, two sets of quantities (i), (ii), and (iv) are obtained from each event by taking each electron in turn with the π^+.

ERRORS

The error $\sigma_{\pi e}$ calculated in the above procedure represents the contribution from only one source of error, viz., the line fitting. It is calculated (see Appendix) that

$$\sigma_{\pi e}^2=(\sigma_\pi^2+\sigma_e^2)\csc^2\theta_{e\pi}-\sigma_\pi^2$$

where the meanings of σ_π and σ_e are given in the Appendix.

A further source of error which is not included in $\sigma_{\pi e}$ is involved in the location of the decay point of the K^+. This point is located *only* on the basis of the single measurement on the estimated end of the K^+ track. Contributions to this error were assumed to be from two sources:

(i) Measurement error due to the subjective choice of the "center" of the final grain in the track;

(ii) an "intrinsic" error due to the true decay point of the K^+ not coinciding with the center of the final grain.

In the following, these errors are denoted by σ_{k1} and σ_{k2}, respectively. σ_{k1} may be expected to be of the same order as the error in a single measurement on a grain, i.e., $\sim 0.05\,\mu$, while σ_{k2} is a consequence of the mechanism of grain formation and the grain size of the emulsion. An estimate of both these errors was obtained from measurements on τ decays of which about 4000 were available in the same stack. Thirty τ's were chosen for measurement having flat tracks and evenly spaced angles between the tracks in order to give maximum accuracy of measurement and subsequent triangulation. The coordinates of the grains in the events were measured in an exactly similar way to the KD events. Three independent measurements of each event were made.

A similar process of line-fitting and geometrical reconstruction as with the KD events is used. The three π tracks intersect in a triangle the centroid of which is taken as the true decay point of the K^+, which can then be compared with the measured position. The general effect observed is illustrated in Fig. 4. This figure presents the results obtained for three measurements on each of nine events.[15] The origin represents the

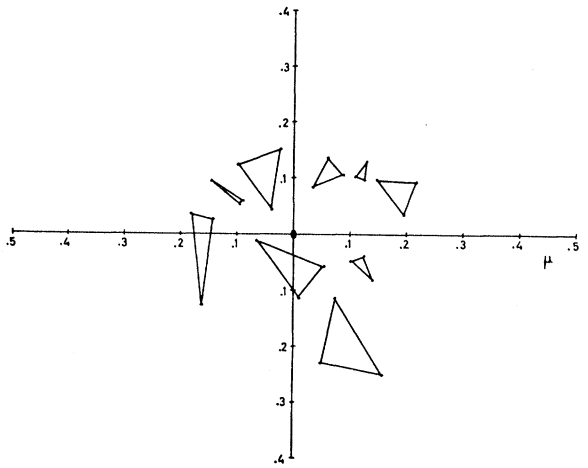

FIG. 4. Positions of measured K^+ decay positions in τ decays. (Coordinates in microns.) The results of 9 events each measured three times are shown; the vertices of each triangle represent the positions of the measured K^+ decay point for the three measurements of a single event, referred to the "true" K^+ decay position (defined from the three secondary π tracks) as origin.

"true" decay point of the K^+ as defined above; the vertices of each triangle represent the measured positions of the K^+ ending for the three separate measurements on one event. The size of each triangle is governed by measurement error, i.e., σ_{k1}, while the displacement of a triangle from the origin may be considered to be due to σ_{k2}, i.e., a property which is constant for measurements on one event. As a result of these observations the following assumptions on the nature of σ_{k1} and σ_{k2} are made:

(i) that the error σ_{k1} is *random* between independent measurements of the same event;

(ii) that the error σ_{k2} is *systematic* for independent measurements of the same event but is *random* between different events.

The measurements on the τ decays are also used to estimate the magnitudes of these two error quantities. One of the π tracks from a τ event is chosen at random as a "pseudo-π^+" leaving the other two as an "electron pair" so that the τ event may be analyzed as though it were a true KD event. It is then known that the "flight distance" of the assumed "π^0" is zero since all three tracks originate from a single center.

We now consider a set of measurements on *one* event either a true KD or a τ which when analyzed give a set of flight distances x_i with corresponding errors $(\sigma_{\pi e})_i$. $\sigma_{\pi e}$ is the error defined previously as being due to the line-fitting procedure and dependent on the angle of intersection of the π^+ and electron tracks. The total random error σ_i in each x_i is therefore given by

$$\sigma_i^2=\sigma_{k1}^2+(\sigma_{\pi e})_i^2.$$

The weighted mean value of x for the set of measure-

[15] The same trend is observed for all the events measured but for clarity they are not all plotted on the diagram.

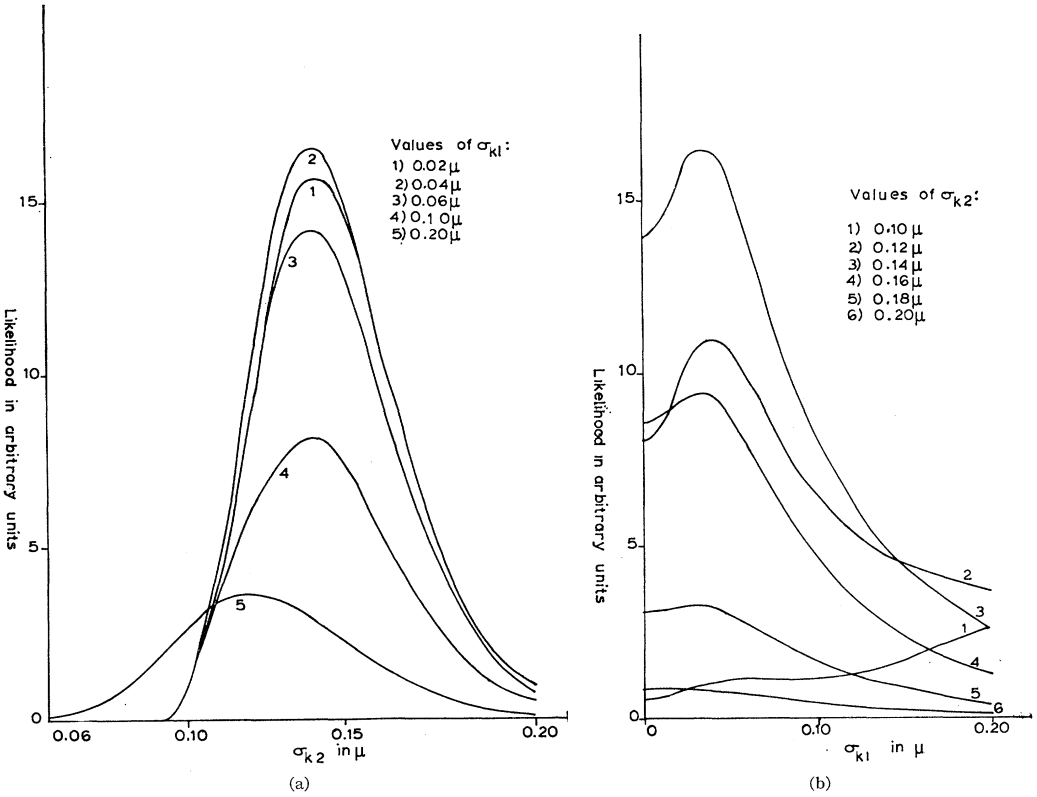

FIG. 5. Likelihood function $L(\sigma_{k1},\sigma_{k2})$ from measurements on τ decays. (a) $L(\sigma_{k2})$ for fixed σ_{k1}; (b) $L(\sigma_{k1})$ for fixed σ_{k2}.

ments on one event is[16]

$$\bar{x}=\sum_i (x_i/\sigma_i^2)/\sum_i (1/\sigma_i^2)$$

with error

$$\sigma^2=1/\sum_i (1/\sigma_i^2).$$

The total error in $\bar{x}$ for the event is then

$$\sigma_{\text{tot}}^2=\sigma_{k2}^2+\sigma^2.$$

In the case of the τ events, the true value of x is known to be zero. We now consider a set of N events for which the values of $\bar{x}$ and σ_{tot} have been computed as described above. For convenience these sets of values will be denoted by X_j and σ_j, respectively, $(j=1,2,\cdots N)$. It is assumed that each X_j is from a population normally distributed about zero mean with a variance σ_j^2, i.e. the distribution function is

$$p(X_j)=\frac{1}{\sigma_j\sqrt{(2\pi)}}\exp(-X_j^2/2\sigma_j^2).$$

It follows therefore that the likelihood function for the observed set of X_j is

$$L(\sigma_{k1},\sigma_{k2})=\prod_{j=1}^{N} p(X_j).$$

(The dependence upon σ_{k1} and σ_{k2} arises because of the dependence of the X_j's and σ_j's upon these quantities.) Maximum-likelihood estimates of σ_{k1} and σ_{k2} can thus be obtained. The likelihood curves calculated from the measurements on the τ events are shown in Fig. 5. It is seen that while σ_{k2} is quite well defined, there is a broader peak for σ_{k1}. This is consistent with the fact that σ_{k2} is determined from the different events (30) while σ_{k1} is only defined from the poor statistics of the 3 measurements on each event. However, a simple calculation indicates that the total error for any event is insensitive to small variations in σ_{k1} so that it was not attempted to obtain a more accurate value. The values chosen from the likelihood curves as reasonable maximum likelihood estimates were $\sigma_{k1}=0.04\,\mu$; $\sigma_{k2}=0.14\,\mu$. These figures are in agreement with the orders of magnitude expected, viz., $\sigma_{k1}\sim 0.05\,\mu$ and $\sigma_{k2}\sim$(the radius of a grain).

Using these values of σ_{k1} and σ_{k2}, a set of values of $\bar{x}$ and σ_{tot} are obtained as described above, for the true KD events measured. These are then corrected for the dip angle of the π^+ track.[17]

ESTIMATION OF LIFETIME

Two estimates of the lifetime are obtained from the experimental data by two different methods, viz., maximum likelihood and weighted mean.

[16] If both electrons are measured, the sums are taken over all the values obtained.

[17] All previous measurements are projected in the plane of the emulsion. In the $K_{\pi 2}$ decay, the π^0 has the same dip as the observed π^+.

The appropriate likelihood function for the situation which includes the exponential decay probability in addition to measurement error is

$$L(\tau)=\prod_{i=1}^{N}\frac{1}{x_0\sigma_i\sqrt{(2\pi)}}\int_0^\infty \exp\left[-\frac{x'}{x_0}-\frac{(x'-x_i)^2}{2\sigma_i^2}\right]dx'$$

($x_0=\beta\gamma c\tau$; $\beta=0.83$ for π^0 in $K_{\pi 2}$ decay at rest), where the data consist of N events with mean measured flight distances x_i and corresponding errors σ_i. The value of τ which maximizes $L(\tau)$ will be denoted by τ_{ml}.

The weighted mean estimate τ_{wm} is given by

$$\tau_{\mathrm{wm}}=\bar{x}/\beta\gamma c,$$

where

$$\bar{x}=\sum_i^N (x_i/\sigma_i^2)\Big/\sum_i^N (1/\sigma_i^2).$$

The results described in the following section are from calculations made on the experimental data from a sample of 58 events from the total of 67. Two of the remaining nine events were rejected as spurious since they gave flight distances of the order of several microns. Investigation of these events revealed that in one case, measurement had been made on an adjacent spurious track, while in the other, one track was very steep (near the dip cutoff imposed in the selection of events for measurement). These two events were abandoned as being unsuitable for measurement. The remaining seven events were measured later and included in the final results quoted.

The results obtained for the 58 events are

$$\tau_{\mathrm{wm}}=0.58\times10^{-16}\ \mathrm{sec};\quad \tau_{\mathrm{ml}}=2.30\times10^{-16}\ \mathrm{sec}.$$

In each case the error is about 0.55×10^{-16} sec. It is clear that these two estimates are inconsistent; they differ by more than 3 standard deviations. The following check is made to test whether such a discrepancy might be expected. Using a technique similar to "Monte Carlo" calculations, a number of samples of ideal "experimental" x_i are concocted assuming, for convenience, a mean lifetime $\tau_{\pi^0}=1.5\times10^{-16}$ sec and including the exponential distribution of lifetime together with a normal distribution with variance σ_i^2. The set of σ_i used is that obtained from the experimental results. Ten such independent samples are made up (although each had the same set of σ_i). From these are obtained the appropriate values of the estimates τ_{ml} and τ_{wm}. The results are shown in Table I where the third column represents the difference between the estimates expressed in units of the standard deviation. (σ_{wm} is the same as previously quoted for the experimental results since the same set of σ_i are used.) It is clear from the table that the discrepancy observed is not to be expected.[18]

[18] There is, however, some indication that $\tau_{\mathrm{wm}}>\tau_{\mathrm{ml}}$ and that there may be an over-all bias to underestimate τ_{π^0}.

TABLE I. Estimates of the mean lifetime by maximum likelihood (τ_{ml}) and by weighted mean (τ_{wm}), for an artificial sample. All lifetimes are in units of 10^{-16} sec.

	τ_{ml}	τ_{wm}	$(\tau_{\mathrm{wm}}-\tau_{\mathrm{ml}})/\sigma_{\mathrm{wm}}$
	0.54	0.68	0.25
	1.63	1.68	0.09
	1.81	1.77	−0.07
	1.27	1.30	0.05
	0.80	1.17	0.67
	1.49	1.63	0.25
	0.55	0.52	−0.05
	1.14	1.23	0.16
	0.55	0.62	0.13
	2.09	1.55	−0.98
Mean	1.19	1.22	

Presence of "Wild Events"

An examination of the experimental values of x_i and σ_i shows that some events are apparently inconsistent with the main set; such events have large flight distances (of either sign) but are attributed with errors too small to account for them. Examples of these events are

x (in μ)	σ (in μ)
−1.21	0.33
−1.26	0.22
1.10	0.24
−1.23	0.27
0.62	0.14 .

Such events are termed "wild."

A simple argument indicates that these wild events have different effects upon the estimate of τ depending upon the method of calculation. With the weighted mean, both positive and negative values are admitted with equal weight (before being weighted by the value of σ_i). It is found that there is a slight excess of negative wild events and hence the value of τ_{wm} is expected to be lower than the true value of τ_{π^0}. The likelihood calculation takes into account the exponential decay distribution and thus negative values of τ (and hence x) are inadmissible unless accompanied with a correspondingly large error. Thus, negative wild events contribute very little to the shape of the likelihood curve whereas positive wild events strongly affect the position of the maximum. Hence τ_{ml} is expected to be greater than the true estimate if wild events are present.

A cutoff criterion is now introduced which rejects events with x_i more than a given number of units of σ_i away from the calculated estimate (x_{wm} or x_{ml} corresponding to τ_{wm} or τ_{ml}). A new estimate of x_{wm} (x_{ml}) is then obtained from the revised set of events. The rejection process is repeated with this new value; all the events are tested including those previously rejected. This process is iterated until the sample of events used for the calculation of x_{wm} (x_{ml}) is not changed after testing. The results of these calculations are given in Table II. It is seen that the exclusion of the wild events achieves the expected agreement between τ_{ml} and τ_{wm}.

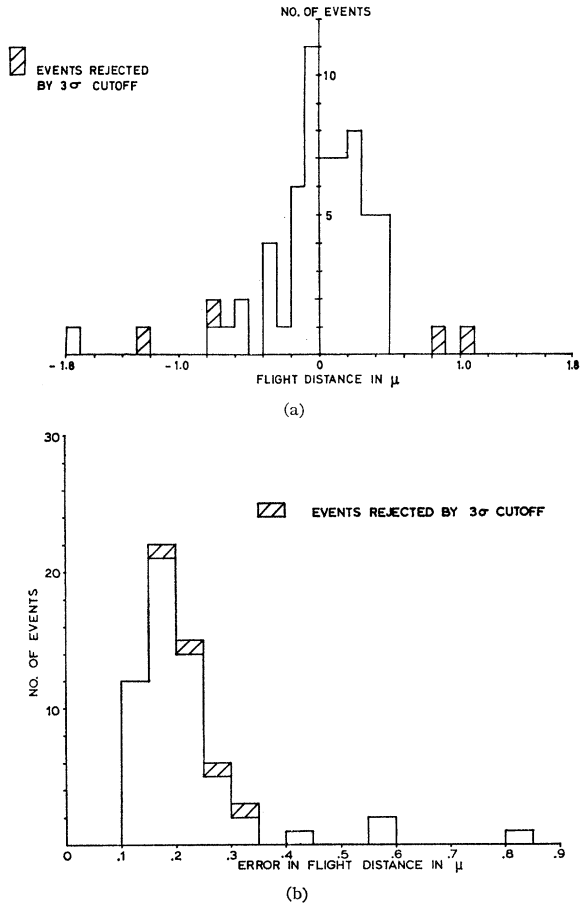

FIG. 6. Observed distributions of (a) flight distance (b) total error in flight distance.

Investigation of the rejected events for the 2.5σ cutoff shows that they can be divided into the following classes:

(i) Both electron tracks measured, but one track consistently giving spurious flight distances for all the independent measurements; (4).

(ii) Four separate measurements inconsistent; (4).

(iii) Very wide angle events ($\theta_{\pi e}\sim 180°$); (1).

(iv) Steep tracks; (1).

(v) Only one electron track measured, giving consistently spurious flight distances; (1).

TABLE II. Results of application of an iterated rejection criterion to eliminate "wild" events. Lifetimes are in units of 10^{-16} sec.

Cutoff	τ_{ml}	No. of events	No. of iterations	τ_{wm}	No. of events	No. of iterations
None	2.30	58	–	0.58	58	–
3σ	1.07	49	1	0.48	51	1
2.5σ	1.25	47	2	1.17	47	1
2σ	1.32	43	2	1.56	43	2

TABLE III. Final results after classification of events and recalculation. Lifetimes are in units of 10^{-16} sec.

Cutoff	τ_{ml}	No. of events	No. of iterations	τ_{wm}	No. of events	No. of iterations
None	2.10	63	–	1.04	63	–
3σ	1.36	59	2	1.17	59	1
2.5σ	1.54	57	3	1.37	58	1
2σ	1.33	52	1	1.61	52	1

The number of events in each class is shown in parentheses.

For the events in class (i), the mean flight distance is recalculated excluding the results from the spurious track. A completely new set of four measurements is made for class (ii) events. The two events in classes (iii) and (iv) are rejected and the remaining event in class (v) is retained to check the effect of a single wild event. At this stage, the seven events previously not included in the calculations are added to the data. This final sample of 63 gives the results shown in Table III, the individual values of x_i and σ_i are given in Table IV where the rejected events are in italics; the distributions of x_i and σ_i are shown in Figs. 6(a) and 6(b), respectively. It is seen that the rejection of only four events by the 3σ cutoff brings the desired consistency between τ_{ml} and τ_{wm}. The variations in τ_{ml} and τ_{wm} caused by the other cutoff criteria are within the total error of about 0.5×10^{-16} sec. The likelihood curves for the complete sample of 63 events and for the sample of 59 events satisfying the 3σ cutoff criterion are shown in Fig. 7. In each case the curve is normalized to $L(\tau_{\mathrm{ml}})=1$. The 3σ cutoff curve drops to $L(0)=0.04$.

Confidence intervals for the lifetime are obtained for both the maximum likelihood and the weighted mean estimates. Use is made of the Bartlett S function for the likelihood method confidence interval.[19,20] The following 90% intervals were obtained from the 3σ cut-off sample:

Maximum likelihood, $(0.58<\tau_{\mathrm{exp}}<2.44)\times 10^{-16}$ sec.

Weighted mean, $(0.30<\tau_{\mathrm{exp}}<2.04)\times 10^{-16}$ sec.

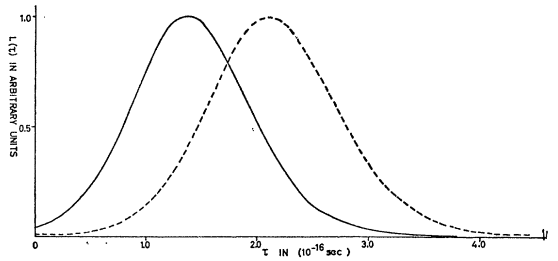

FIG. 7. Likelihood function $L(\tau)$, for complete sample of 63 events: ----; for sample of 59 events left after 3σ cutoff: ———.

[19] M. S. Bartlett, Phil. Mag. 44, 249 (1953).

[20] The formulas quoted by Orear [University of California Radiation Laboratory Report UCRL-8417, p. 18 (unpublished)] are used.

CORRECTION FOR CONTAMINATION EVENTS

As was mentioned previously, a correction to the final value of lifetime is required due to the presence of contamination events involving three-body decay modes of K^+ ($K_{\mu 3, e3}$). In these three-body decays the direction and momentum of the π^0 is not unique but the events present are analyzed as a $K_{\pi 2}$ decay and hence contribute a false lifetime estimate. A possible configuration for a contamination event is shown in Fig. 8. For the good-geometry events[21] (which receive most weighting) the calculated flight distance x of the π^0 is approximately equal to the projection of the true flight distance on to the line of flight of the μ^+ (e^+). The mean value of x for all events of one type ($K_{\mu 3}$ or K_{e3}) is given by

$$\bar{x}=\frac{c\tau_\pi}{m_\pi}\int_0^{p\max} dp\int_{-\pi}^{\pi} d\theta\int_0^{2\pi} d\phi\; pf(p,\theta)\cos\theta\sin\theta,$$

where $f(p,\theta)dpd\Omega$ is the momentum distribution of the π^0 from the K^+ decay (calculated from phase-space considerations); $p_{\max}$ is the maximum momentum of the π^0; m_π and τ_π are the mass and mean life of the π^0, respectively.[22]

If the event is treated as a $K_{\pi 2}$ decay, it is assumed that

$$\tau_f=\bar{x}/(\beta\gamma)_{\pi 2}c,$$

where $(\beta\gamma)_{\pi 2}$ is appropriate for the π^0 emitted in $K_{\pi 2}$ decay and τ_f is the "false" value of lifetime obtained from contamination events. The results of this calculation give

$$\tau_f=0.50\tau_\pi \quad \text{for} \quad K_{\mu 3} \text{ decays}$$
$$=0.39\tau_\pi \quad \text{for} \quad K_{e3} \text{ decays.}$$

Combining these results according to the relative branching ratios,

$$K_{\pi 2}:K_{\mu 3}:K_{e3}=0.77:0.09:0.14,$$

the relation $\tau_\pi=1.15\,\tau_{\exp}$ is obtained where $\tau_{\exp}$ is the value of the experimental lifetime. The correction factor does not affect the width of the confidence interval. The corrected results are:

Maximum likelihood: $\tau_{\pi^0}=(1.56_{-0.5}{}^{+0.6})\times10^{-16}$ sec,
or $P(0.78\times10^{-16}<\tau_{\pi^0}<2.64\times10^{-16})=90\%$

Weighted mean: $\tau_{\pi^0}=(1.34\pm0.53)\times10^{-16}$ sec,
or $P(0.47\times10^{-16}<\tau_{\pi^0}<2.21\times10^{-16})=90\%$.

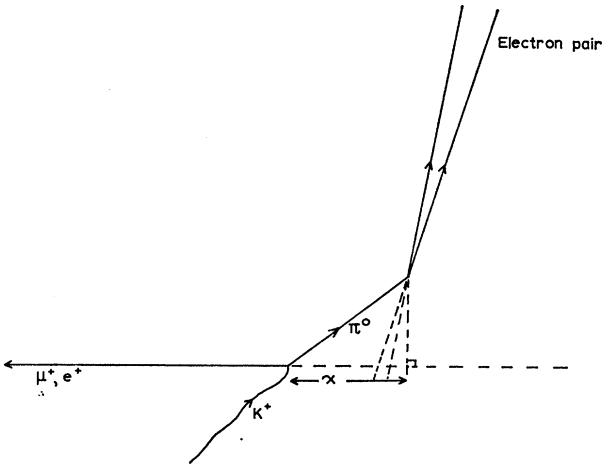

FIG. 8. Geometry of possible contamination event.

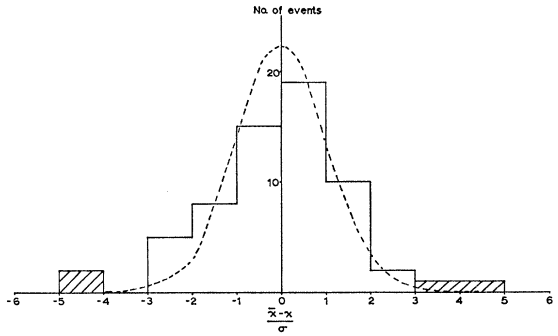

FIG. 9. Distribution of $(\bar{x}-x_i)/\sigma_i$ for all events. $\bar{x}$ is flight distance corresponding to $\tau_{\rm ml}=1.36\times10^{-16}$ sec. Shading denotes events rejected by 3σ cutoff.

As a test of the estimation of the experimental errors (σ_i) the distribution of $(\bar{x}-x_i)/\sigma_i$ is plotted in Fig. 9. ($\bar{x}$ is the flight distance corresponding to the uncorrected value of $\tau_{\rm ml}=1.36\times10^{-16}$ sec.) If the error estimations are reasonable, the distribution should be approximately normal, with zero mean and unit variance. The dashed curve in the figure indicates this distribution. Serious errors in the calculation of the σ_i's would alter the variance from unity but it is seen that the fit is quite good if the wild events are excluded.

ACKNOWLEDGMENTS

The author wishes to thank Dr. Lofgren and his staff at the Berkeley Bevatron for the facilities for exposure of the stack. Special thanks are due to Dr. J. H. Mulvey for supervising the exposure, being responsible for a great deal of the preliminary exploratory work on the method, and for continuing advice and interest in the progress of the whole experiment. The encouragement and interest shown by Professor D. H. Wilkinson have been greatly appreciated. The author is very grateful for helpful discussions with Dr. S. Lokanathan and Dr. Y. Prakash and for preliminary development work on the digitized eyepiece by Dr. F. Foster. Finally the indispensible aid of the scanners of the Oxford emulsion group is cordially acknowledged, as is the support provided by the D.S.I.R. to the author.

[21] I.e., $\theta_{\pi e}\sim90°$.
[22] For simplicity the mean life is used instead of a distribution.

APPENDIX

A. Calculation of Intersection Error Expression

It is assumed that each fitted line is constrained to pass through the "centroid" of the measured grain coordinates[23] but that due to the spread of the coordinates about a straight line, the calculated gradient (m) of the line has an error δm.

In Fig. 10 the full lines represent the true positions of

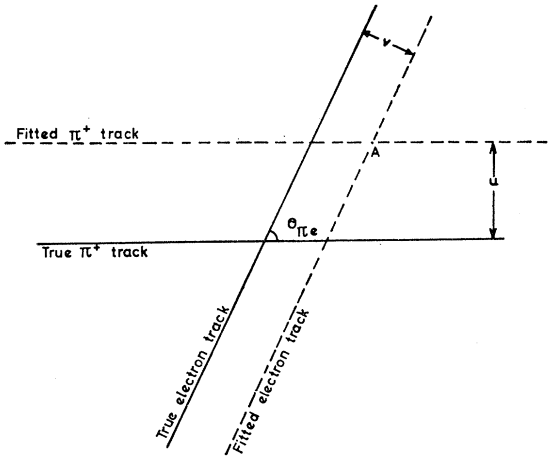

FIG. 10. Illustration of effect at intersection of tracks subject to fitting error.

the tracks while the dotted lines indicate possible fitted tracks. The centroids of the coordinates for each track are sufficiently distant so that the effect of δm is to displace the fitted lines but maintain parallelism with the true tracks. The perpendicular displacements are denoted by u and v. It is assumed that u and v are normally distributed about the true track positions with standard deviations σ_π and σ_e, respectively. If the true tracks are taken as axes of an oblique coordinate system, the point of intersection of the fitted lines (A) may be assigned coordinates (u,v). It follows that the probability that the calculated intersection point (A) lies in an element of area $dudv$ about (u,v) is

$$p(u,v)dudv=C\exp\{-\tfrac{1}{2}(u^2/\sigma_\pi^2+v^2/\sigma_e^2)\}dudv,$$

where C is a constant such that $p(u,v)$ is normalized to unity over the whole (u,v) plane. Orthogonal axes are now taken with the same origin and with the x axis along the π^+ track. The transformation is $u=y$; $v=(\alpha x-y)/(1+\alpha^2)$, where $\alpha=\tan\theta_{\pi e}$. The probability distribution becomes

$$p'(x,y)dxdy=p(u,v)\alpha(1+\alpha^2)^{-1/2}dudv.$$

The probability distribution appropriate to the determination of the flight distance is given by the marginal distribution of x:

$$p''(x)dx=\int_{-\infty}^{\infty}p'(x,y)dydx.$$

The calculation shows that $p''(x)$ is a normal distribution with zero mean (i.e. there is no bias in the location of the decay point of the π^0) and a variance σ^2 given by

$$\sigma^2=(\sigma_\pi^2+(1+\alpha^2)\sigma_e^2)/\alpha^2$$
$$=(\sigma_\pi^2+\sigma_e^2)\csc^2\theta_{\pi e}-\sigma_\pi^2.$$

Hence σ is the required error in the flight distance due to the line-fitting and the intersection angle of the tracks.

The error in the gradient of a track (δm) is calculated from

$$(\delta m)^2=\left[\sum_{i=1}^{N}x_i^2\sum_{i}^{N}y_i^2-\left(\sum_{i}^{N}x_iy_i\right)^2\right]\Big/\left[(N-2)\sum_{i}^{N}x_i^2\right],$$

where N is the number of co-ordinates. As it stands, this expression is only applicable for the usual least squares fit which assumes no error in x. This situation may be obtained in the present case by rotating the coordinate axes so that the track lies along the new x' axis.

The values of σ_π and σ_e are given by the relations $\sigma_{\pi,e}=r_{\pi,e}\delta m_{\pi,e}$, where $r_{\pi,e}$ is the distance from the

TABLE IV. Individual values of x_i and σ_i in μ. Italicized events are those rejected by a 3σ cutoff criterion.

x	σ	x	σ
0.37	0.81	−0.07	0.22
−0.32	0.16	0.30	0.57
−0.34	0.17	0.44	0.22
0.13	0.14	−1.80	2.30
−0.65	0.33	−0.72	0.56
0.20	0.15	−0.21	0.40
−0.03	0.26	0.41	0.20
0.22	0.15	−0.05	0.16
−0.17	0.21	−0.00	0.20
−0.51	0.34	−0.11	0.24
0.21	0.25	*1.10*	*0.24*
0.21	0.19	0.21	0.19
0.09	0.16	0.30	0.16
0.21	0.15	−0.17	0.21
0.18	0.15	−0.15	0.27
0.13	0.18	−0.16	0.15
−0.08	0.18	−0.09	0.16
0.12	0.15	−0.09	0.14
0.48	0.23	0.20	0.26
0.05	0.15	0.32	0.16
0.07	0.19	0.45	0.18
0.08	0.16	0.09	0.14
0.08	0.15	−0.03	0.14
−0.06	0.14	−0.17	0.17
0.33	0.16	0.11	0.16
−0.02	0.24	0.05	0.27
−0.75	*0.17*	0.20	0.21
−1.28	*0.33*	−0.34	0.24
−0.10	0.21	0.14	0.21
0.39	0.14	*0.84*	*0.25*
0.08	0.14	−0.57	0.25
−0.39	0.17		

[23] In the line fitting procedure, this constraint is also applied to reduce the number of unknowns; it is justified since it can be shown that the best fit always passes through the centroid.

centroid of the coordinates of the π (electron) track to the point of intersection of the tracks.

B. Causes of "Wild" Events

The values of x and σ for the four wild events excluded from the final sample of events are italicized in Table IV. Possible causes for these figures are

(i) that the first grain of one of the secondary tracks was formed so close to the K^+ ending as to be indistinguishable from the true end of the track,

(ii) that the electron or π^+ suffers a single scatter near the K^+ ending; if this took place before the first grain of the track were formed, it could not be detected.

The cause (i) does not seem to be possible as the grain diameter is only $\sim 0.3\,\mu$. The second possibility appears the more reasonable especially when the other events are considered in which only one of the electron tracks gave a wild result while the other was well behaved.

PHYSICAL REVIEW VOLUME 139, NUMBER 4B 23 AUGUST 1965

Direct and Y_1^*-Resonant Production of Λ^0 and π^- and Σ-Λ^0 Conversion Following $\bar{K}$-Meson Nuclear Absorption. Final-State Interactions in the $\bar{K}+{}^4\mathrm{He} \rightarrow \pi^- + \Lambda^0 + {}^3\mathrm{He}$ Reaction

P. SAID AND J. SAWICKI
Laboratoire Joliot-Curie de Physique Nucléaire, Orsay (Seine et Oise) France
(Received 7 April 1965)

In the reaction of $\bar{K}$-meson nuclear absorption, three fundamental processes are considered: a direct (nonresonant) $\bar{K}+N \rightarrow \pi^-+\Lambda^0$ reaction, the same reaction with the Y_1^* resonance formation in the intermediate state, and the reaction with a Σ production in the first stage and its subsequent conversion into a Λ^0 in a successive collision with another nucleon. The "zero-range" impulseapproximation is assumed. The initial $\bar{K}$ state is an nS or an mP Bohr mesoatomic orbit. Several forms of the Λ^0-nucleus final-state interaction are considered. For the case of the $\bar{K}+{}^4\mathrm{He} \rightarrow \pi^-+\Lambda^0+{}^3\mathrm{He}$ reaction the recoiling-^{3}He momentum distribution, the pion momentum distribution, and the $\pi^-+\Lambda^0$-^{3}He angular distribution are analyzed. It turns out that in order to explain the ^{3}He momentum distribution no elastic scattering distortion of the Λ^0-^{3}He wave is sufficient, and one has to introduce the Σ-Λ^0 conversion amplitude, which is most important at high ^{3}He-momenta, and which also improves our pion momentum distribution.

1. INTRODUCTION

IN a previous paper by one of us[1] the reaction $\bar{K}+{}^4\mathrm{He} \rightarrow \pi^-+\Lambda^0+{}^3\mathrm{He}$ has been studied. Such a reaction is important for the study of the mechanism of the absorption of $\bar{K}$ mesons in nuclei and for the study of final-state interactions, especially of the outgoing hyperon-nucleus interaction. In I the formation of the Y_1^* resonance in the intermediate state is assumed to be the most important absorption mechanism, in contrast to some previous publications listed in that reference. This assumption helps us to understand fairly well the position of the maximum of $R_3(p_3)$, the distribution of the reaction rate as a function of the momentum p_3 of the recoiling ^{3}He nucleus. Another distribution function $R_\pi(p_\pi)$ of the reaction rate as a function of the outgoing pion momentum p_π is rather model-insensitive.

In explaining the function $R_3(p_3)$, however, neither the far-off tail (large p_3) of the experimental histogram[2] nor even the region of less small p_3 can be understood well. It was speculated in I that the discrepancies mentioned could be accounted for by introducing a really correct nuclear wave function (form factor) and/or by a proper treatment of the final-state interaction (the elastic-scattering Λ-^{3}He distortion). Indeed, neither of these two points has been satisfactorily treated in I. It will be seen from the present analysis, however, that neither of these two speculations of I and of other papers is correct, i.e., that neither of these two effects alone nor both of them combined suffice to explain the observed $R_3(p_3)$.

It turns out, indeed, that it is necessary to consider the Σ-Λ conversion amplitude as an extra component, and actually as a combined effect of the three generally interfering components: (1) a direct (nonresonant) amplitude, (2) a Y_1^* resonance amplitude, and (3) a direct Σ-production t-matrix element with the (second-stage) Σ-Λ conversion amplitude (or, equivalently, an

[1] J. Sawicki, Nuovo Cimento **33**, 361 (1964) referred to hereafter as I.

[2] Helium Bubble Chamber Collaboration Group, Nuovo Cimento **20**, 724 (1961); J. Auman, *et al.*, *Proceedings of the 1962 Annual International Conference on High-Energy Nuclear Physics at CERN*, edited by J. Prentki (CERN, Geneva, 1962), p. 330; cf., also *Proceedings of the 1960 Annual International Conference on High-Energy Physics at Rochester*, edited by E. C. G. Sudarshan, J. H. Tincot, and A. C. Melissions (Interscience Publishers, Inc., New York, 1960), p. 426.